Supplementary Information

Psoriasis-associated variant Act1 D10N with impaired regulation by Hsp90

Supplementary Figure 1

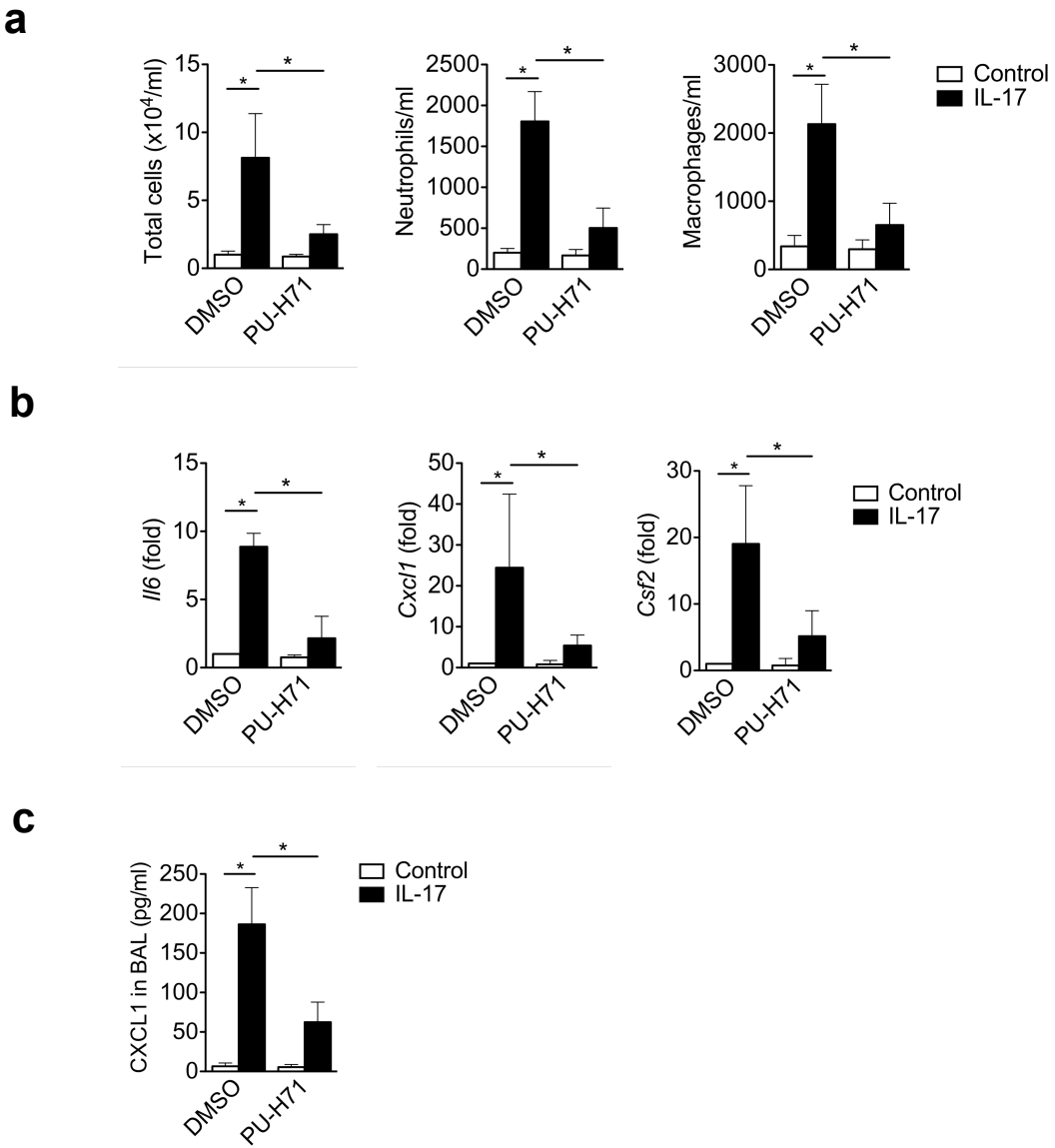

Supplementary Figure 1. Hsp90 inhibitor attenuates IL-17-mediated pulmonary inflammation. **(a)** Total BAL cell and differential cell counts from DMSO or PU-H71 pretreated mice (75mg/kg of inhibitor injected intraperitoneally, once daily for two days before IL-17 injection) left unchallenged (Control) or challenged for 24 h by intranasal injection of IL-17 (1μg). Data are graphed as mean fold induction over unchallenged ± SEM. **(b)** Lung tissues isolated from mice treated as in **(a)** were subjected to RT-PCR analysis for *Il6*, *Cxcl1*, and *Csf2* induction. **(c)** ELISA assay for CXCL1 in BAL fluid from mice treated as in **(a)**. *$p < 0.05$ (Student's *t*-test). Data are representative of two independent experiments with 6 mice per group.

Supplementary Figure 2

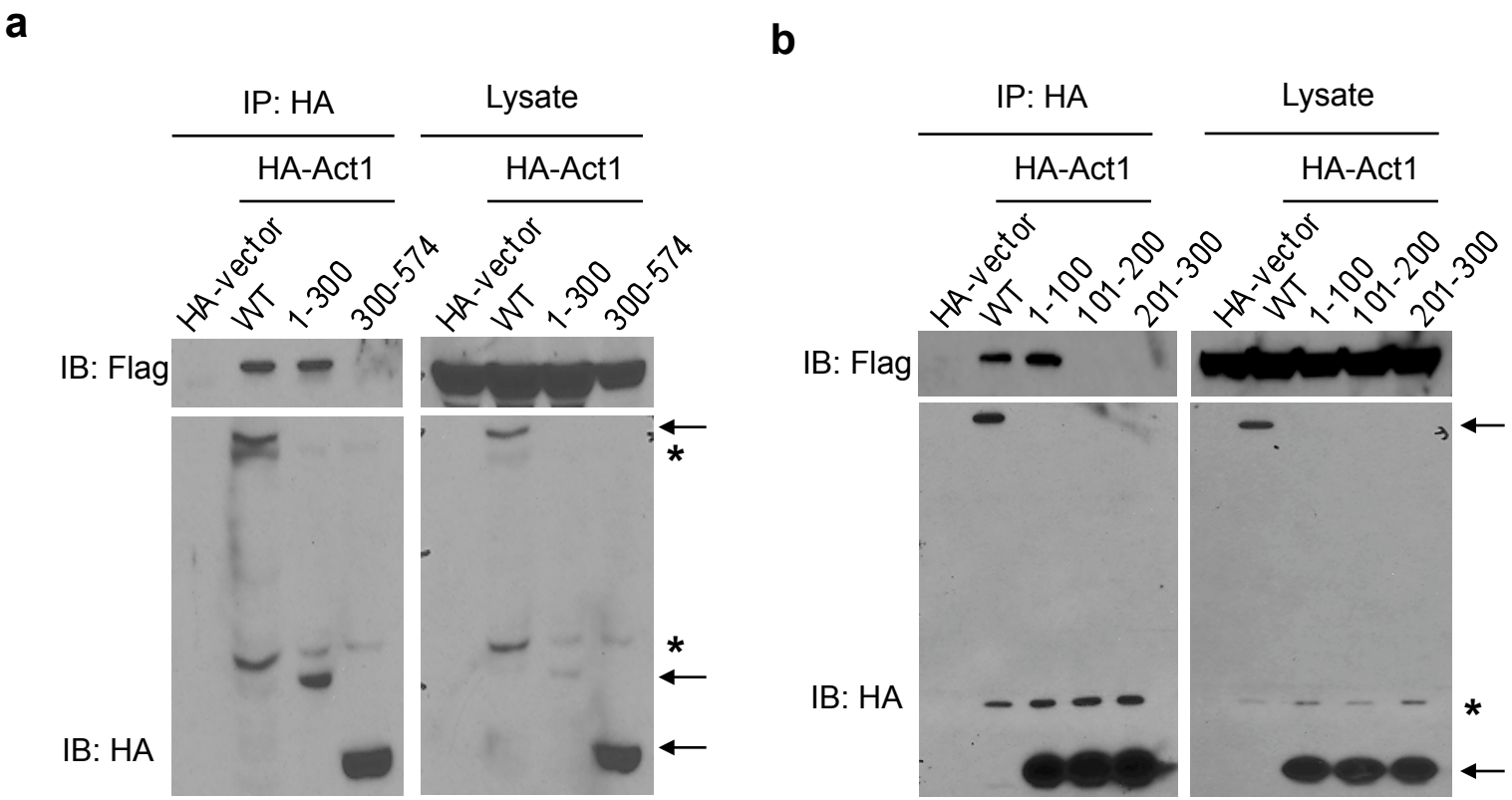

Supplementary Figure 2. Act1 1-100 is sufficient to interact with Hsp90. **(a)** HEK293 cells were transiently transfected with Flag-Hsp90 plus HA-vector, HA-Act1 WT, HA-Act1 1-300, or HA-Act1 300-574. Cell lysates were immunoprecipitated with anti-HA, followed by immunoblot analysis for Flag and HA. Arrows indicate Act1. Asterisks indicate non-specific bands. **(b)** HEK293 cells were transiently transfected with Flag-Hsp90 plus HA-vector, HA-Act1 WT, HA-Act1 1-100, HA-Act1 101-200, or HA-Act1 201-300. Cell lysates were immunoprecipitated with anti-HA, followed by immunoblot analysis for Flag and HA. Arrows indicate Act1. Asterisks (*) denote none-specific bands. Data are representative of two independent experiments.

Supplementary Figure 3

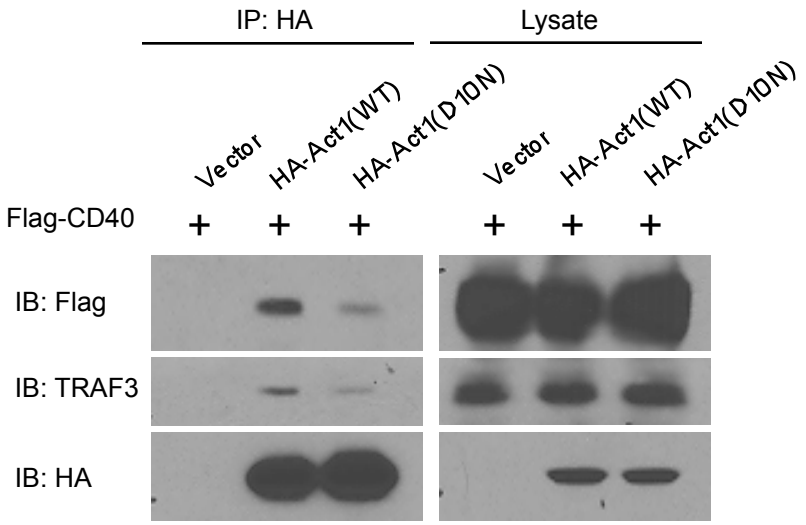

Supplementary Figure 3. Loss of interaction between Act1 (D10N) and CD40. HEK293 cells were transiently transfected with Flag-CD40 plus HA-vector, HA-Act1 WT or HA-Act1 (D10N). Cell lysates were immunoprecipitated with anti-HA, followed by immunoblot analysis for Flag, TRAF3 and HA. Data are representative of two independent experiments.

Supplementary Figure 4

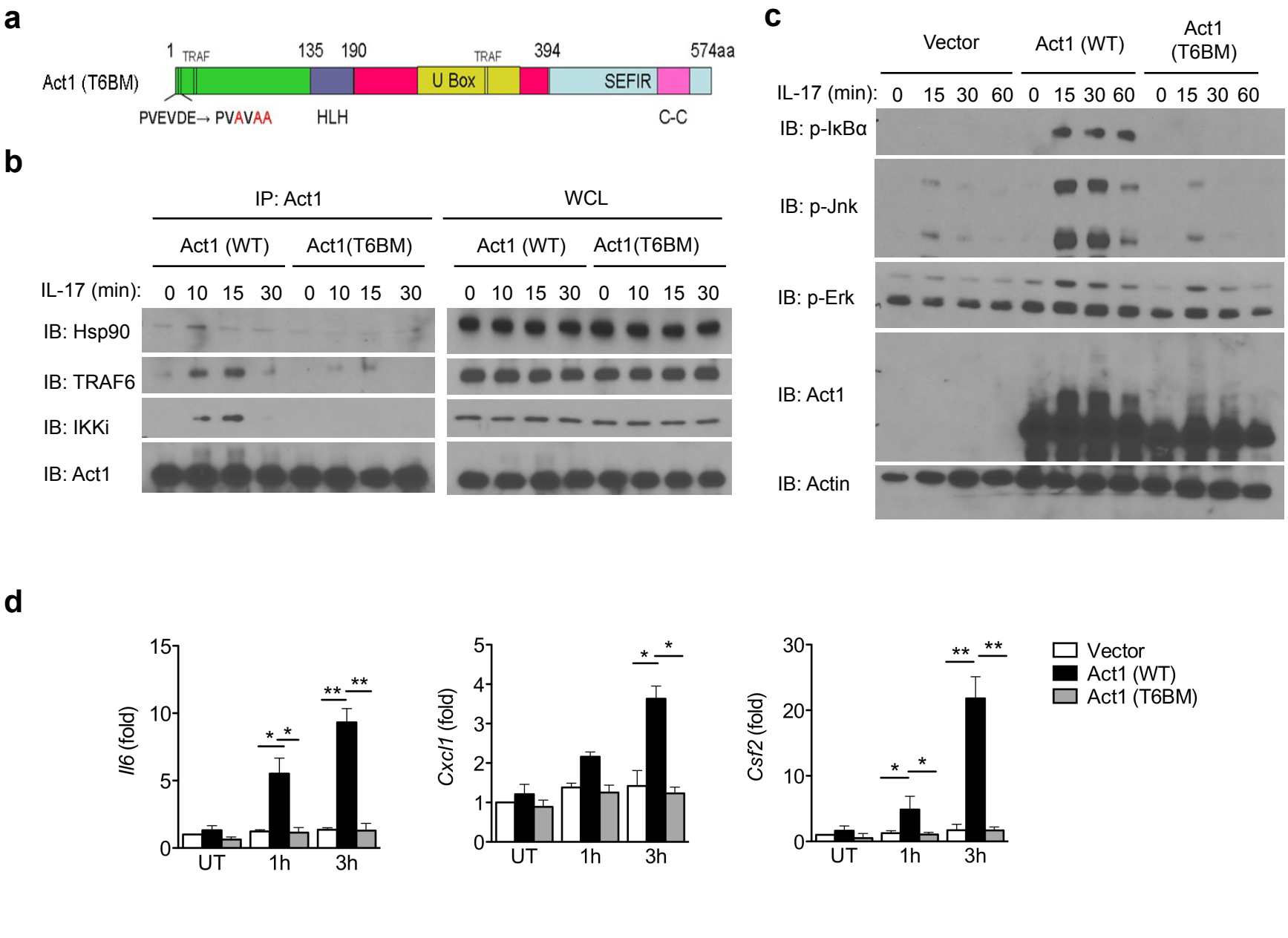

Supplementary Figure 4. Act1 (T6BM) is a loss-of-function mutant. **(a)** Schematics of Act1 (T6BM) mutation (PVEVDE→ PVAVAA). **(b)** *Act1*$^{-/-}$ MEFs transduced with Act1 (WT) or Act1 (T6BM) were treated with IL-17 (50 ng/ml) for the indicated times. Cell lysates were immunoprecipitated with anti-Act1, followed by immunoblot analysis for Hsp90, TRAF6, IKKi and Act1. **(c)** *Act1*$^{-/-}$ MEFs transduced vector, Act1 (WT) or Act1 (T6BM) were treated with IL-17 (50 ng/ml) for the indicated times, followed by immunoblot analysis. **(d)** *Act1*$^{-/-}$ MEFs tranduced as in **(c)** were treated with IL-17 (50 ng/ml) for the indicated times followed by RT-PCR analysis for *Il6*, *Cxcl1* and *Csf2* induction. Untreated (UT). *$p < 0.05$, **$p < 0.01$ (Student's *t*-test). Data are representative of three independent experiments.

Supplementary Figure 5

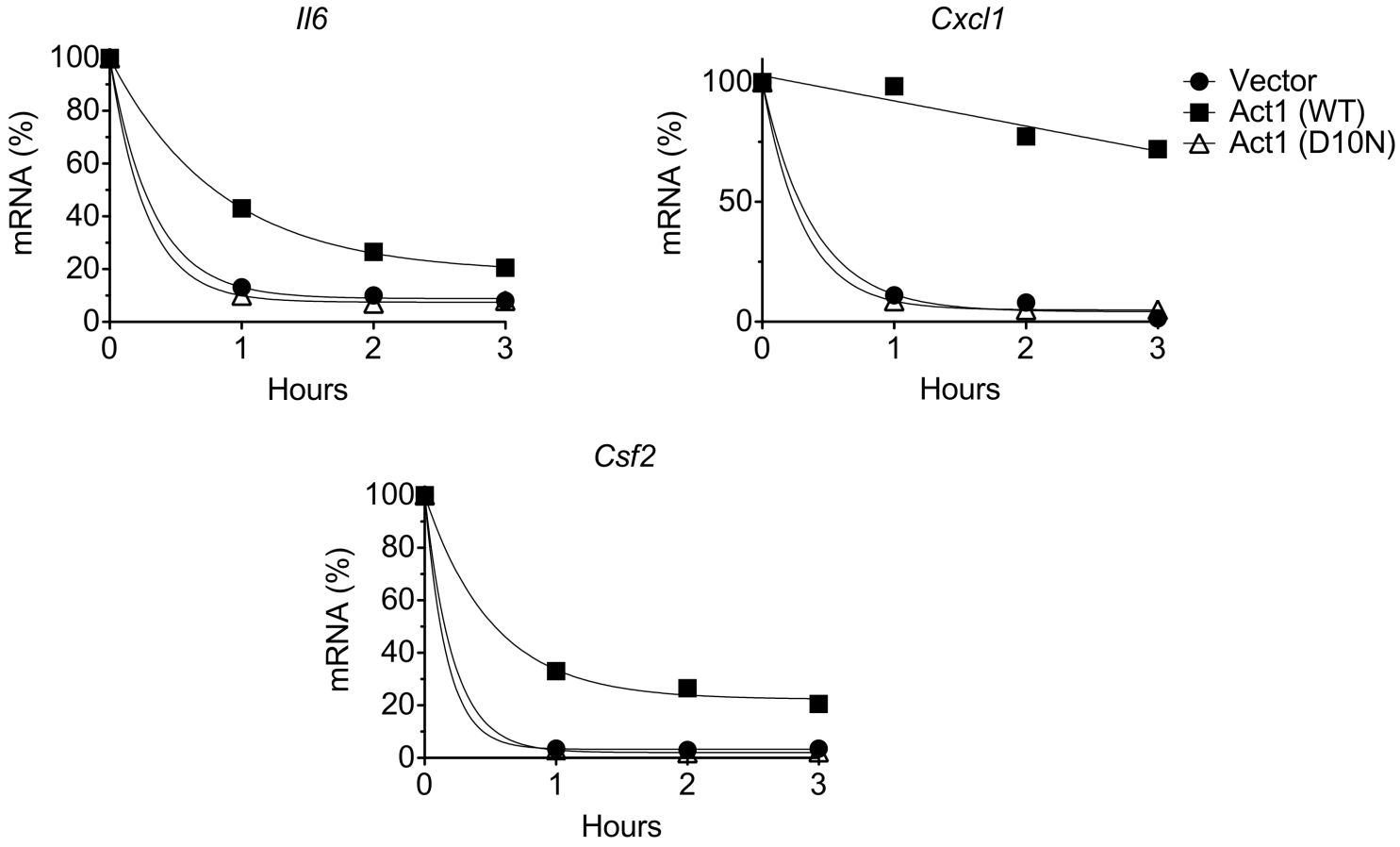

Supplementary Figure 5. Loss of mRNA stability in Act1 (D10N). *Act1*$^{-/-}$ MEFs were transduced with vector, Act1 (WT), or Act1 (D10N) and pretreated with TNF (10ng/ml) for 1 hour. Cells were then treated with IL-17 (50ng/ml) and actinomycin D (ActD) (5μg/ml) for the indicated times followed by RT-PCR analysis for *Il6*, *Cxcl1*, and *Csf2* expression. Gene expression prior to IL-17 and ActD treatment was defined as 100%. mRNA stability is defined as the percentage of mRNA that remains after Act1D treatment. Data are one representative of three independent experiments.

Supplementary Figure 6

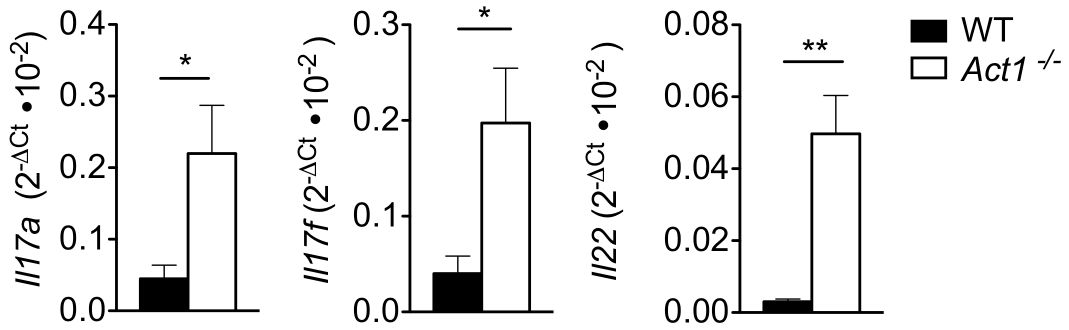

Supplemental Figure 6. RT-PCR analysis of *Il17a, Il17f,* and *Il22* transcripts in the lymph nodes of 6 weeks old Act1 WT or *Act1*$^{-/-}$ mice (n= 5 per group). *$p < 0.05$, **$p < 0.01$ (Student's *t*-test). Data are from three independent experiments.

Supplementary Figure 7

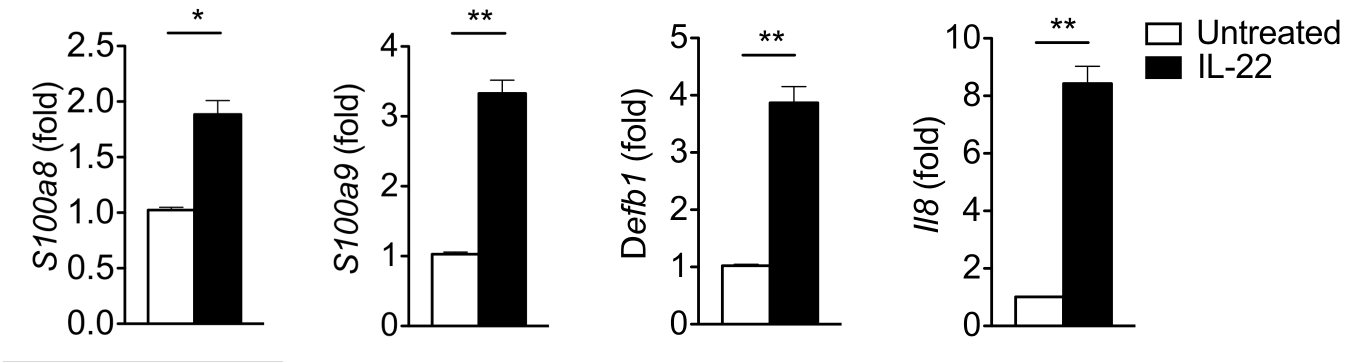

Supplementary Figure 7. RT-PCR analysis of *S100a8, S100a9, Defb1* and *Il8* expression in human keratinocytes treated with IL-22 (50ng/ml) for three hours. Data are presented as fold induction over untreated. *$p < 0.05$, **$p < 0.01$ (Student's *t*-test). Data are representative of two experiments.

Supplemental Figure 8

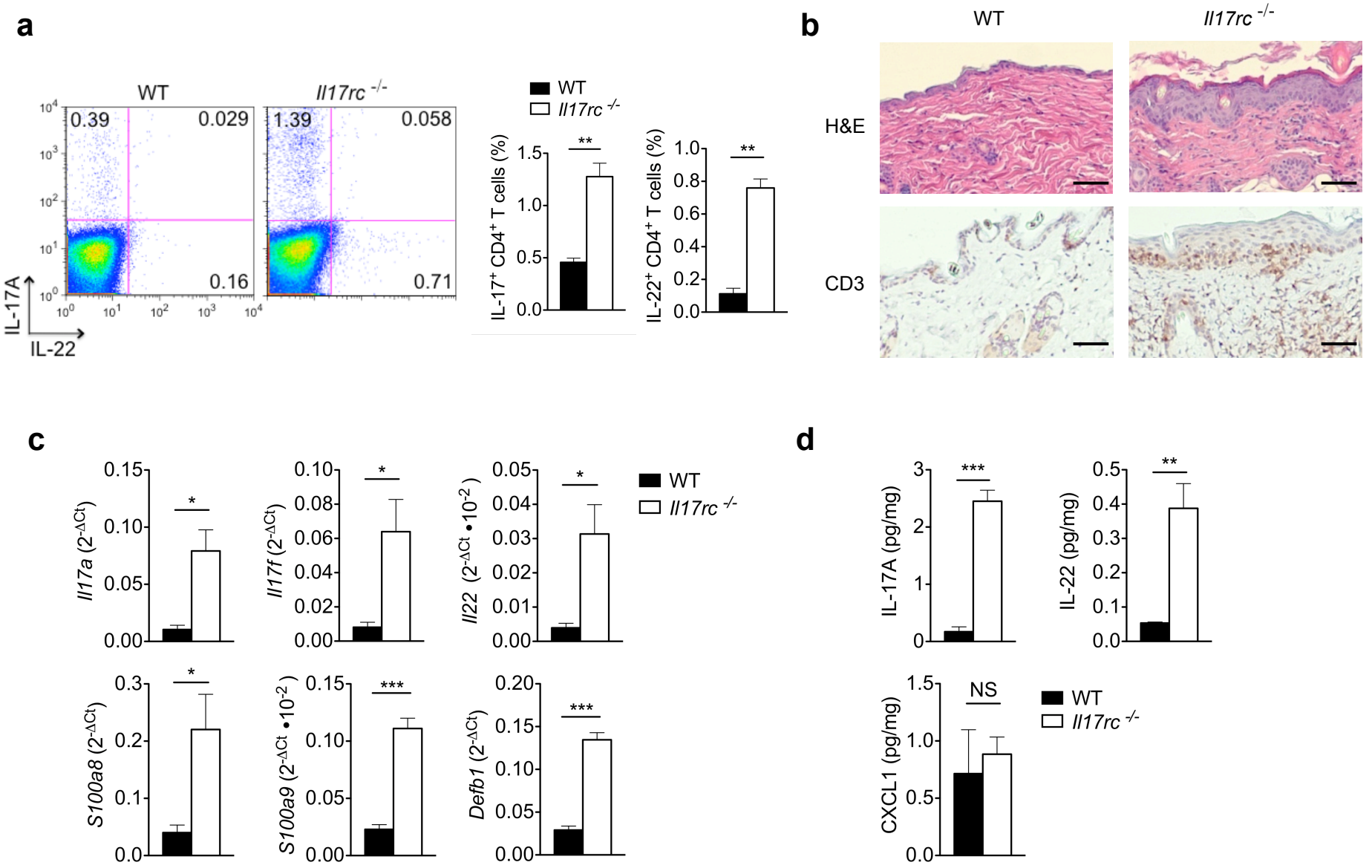

Supplemental Figure 8

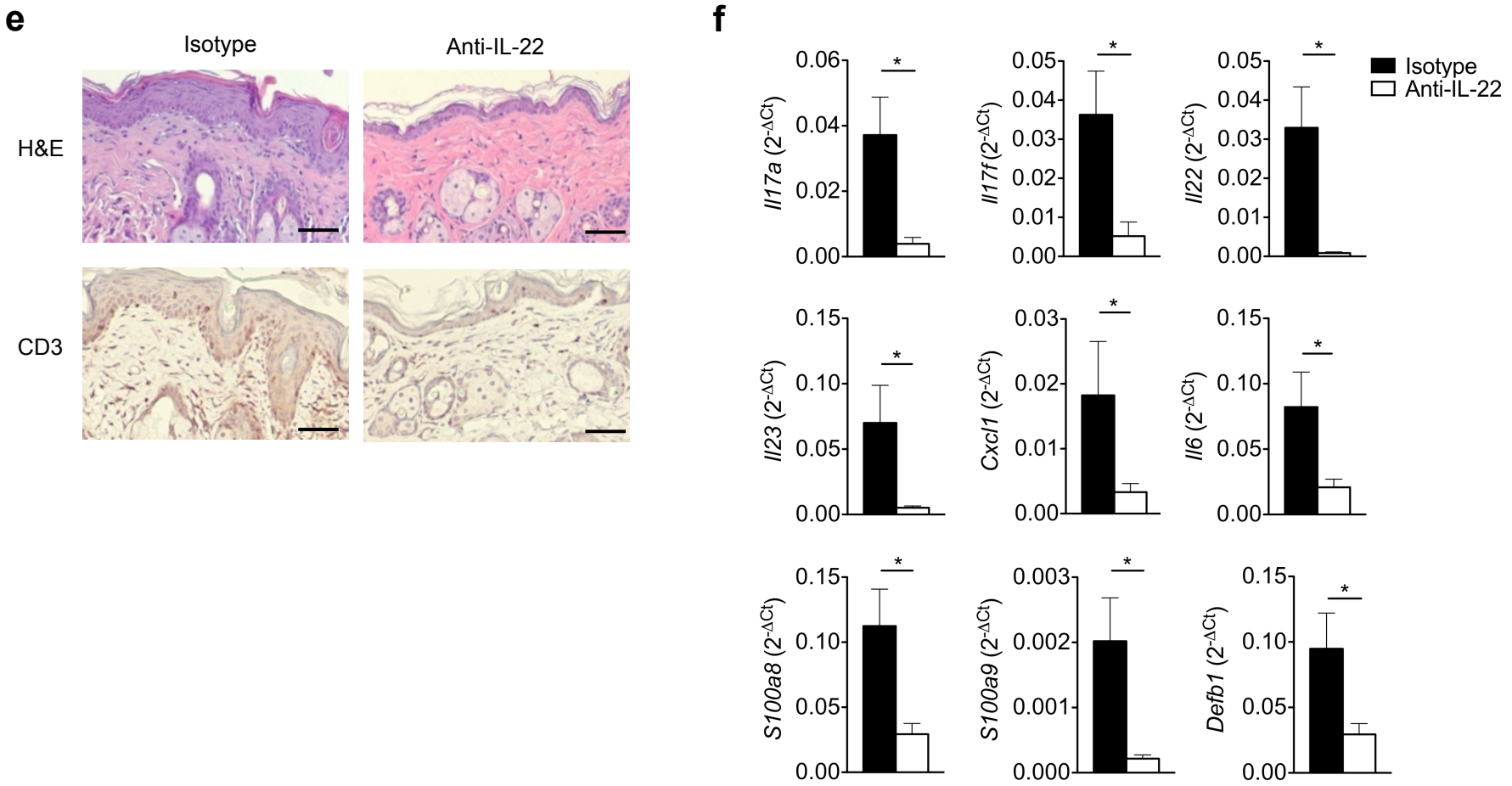

Supplementary Figure 8. Skin inflammation in *Il17rc*$^{-/-}$ mice. **(a)** Cells were isolated from the lymph nodes of WT or *Il17rc*$^{-/-}$ mice and stimulated with PMA and ionomycin for 5 hours followed by intracellular staining for IL-17 and IL-22**.** Flow plots are gated on CD4^{+} T cells. Right graph indicates the percentage of IL-17^{+} and IL-22^{+} CD4^{+} T cells. **(b)** Skin sections from WT or *Il17rc*$^{-/-}$ mice stained with H&E or with anti-CD3. Scale bar indicates 50μm. **(c)** RT-PCR analysis of gene transcripts the skin of WT or *Il17rc*$^{-/-}$ mice. Data are graphed as mean $2^{-\Delta Ct}$ ± SEM. **(d)** Cytokine production by skin infiltrates isolated from the skin of WT and *Il17rc*$^{-/-}$ mice. Cytokine production was normalized to tissue weight. **(e)** Skin sections from isotype or anti-IL-22-treated *Il17rc*$^{-/-}$ mice were stained with hematoxylin and eosin or with anti-CD3. Scale bar indicates 50μm. **(f)** RT-PCR analysis of cytokine transcripts in the skin of isotype or anti-IL-22-treated *Il17rc*$^{-/-}$ mice. *$p < 0.05$, **$p < 0.01$, ***$p < 0.005$, not significant (NS) (Student's *t*-test). Data are representative of two independent experiments.

Supplementary Figure 9

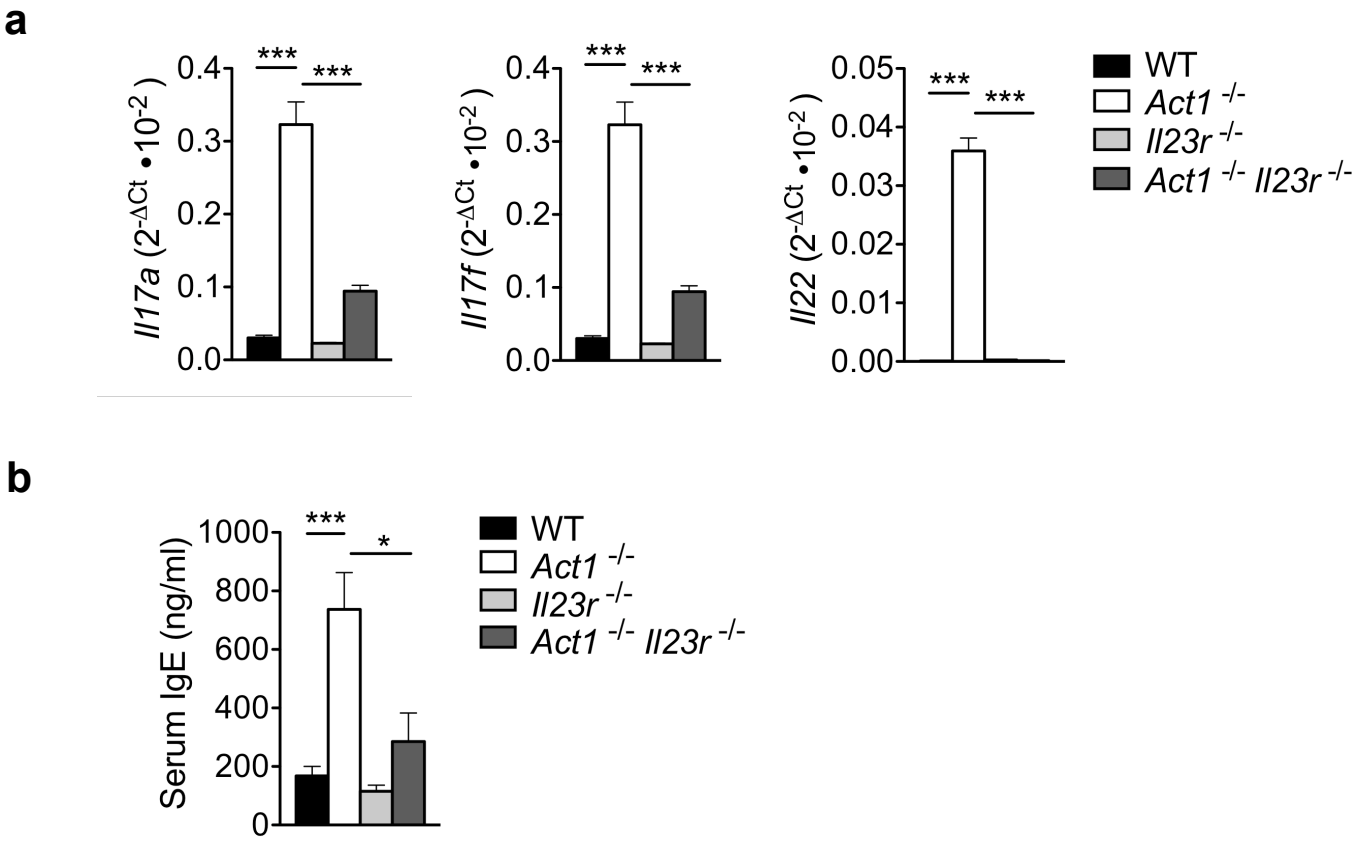

Supplementary Figure 9. Loss of IL-23 signaling attenuates the hyper T_H17 response in *Act1*$^{-/-}$ mice. (**a)** RT-PCR analysis of *Il17a, Il17f,* and *Il22* transcripts in the lymph nodes of 6 weeks old WT, *Act1*$^{-/-}$, *Il23r*$^{-/-}$, and *Act1*$^{-/-}$ *Il23r*$^{-/-}$ mice. **(b)** Serum IgE levels of WT, *Act1*$^{-/-}$, *Il23r*$^{-/-}$, and *Act1*$^{-/-}$ *Il23r*$^{-/-}$ mice at 6mos of age. *$p < 0.05$, ***$p < 0.005$ (Student's *t*-test). Data are representative of two independent experiments.